Transformations for Estimating Body Surface Potential Maps from the Standard 12-Lead Electrocardiogram

John J Wang[1], John L Sapp[2], James W Warren[2], B Milan Horáček[2]

[1]Philips Healthcare, Andover, MA, USA; [2]Dalhousie University, Halifax, NS, Canada

Abstract

The aim of this study was to compare general and patient-specific transformations for estimating body surface potential maps (BSPMs) from the standard 12-lead electrocardiogram (ECG). The design set for deriving the general transformation consisted of 120-lead BSPMs of Dalhousie Superset (n = 892); as a test set for comparing patient-specific and general transformations we used 120-lead BSPMs from the Dalhousie database of patients (n = 88) who underwent elective percutaneous coronary intervention (PCI). From these two datasets we derived the desired transformations by regression analysis. The estimated BSPMs were assessed by 3 goodness-of-fit measures: similarity coefficient (*SC*), root-mean-square error, and relative error (*RE*). Results show that BSPMs can be estimated from the 12-lead ECG by using general transformation with (mean ± SD) *SC* (%) = 92.4 ± 3.5 and *RE* (%) = 42.2 ± 9.2; patient-specific transformations yielded significantly better (P < 0.0001) estimates, achieving *SC* (%) = 96.6 ± 4.3 and *RE* (%) = 22.4 ± 10.7. Thus, in conclusion, BSPMs of our particular test set could be estimated from the standard 12-lead ECG with a very good accuracy by means of general transformation. With patient-specific transformations, accuracy was further improved. In patient monitoring and some clinical interventional procedures (e.g., elective PCI, catheter ablation), a pre-procedure BSPM recording can be used to derive patient-specific lead transformation that can subsequently enhance utility of the 12-lead ECG during the procedure.

1. Introduction

Electrocardiographic monitoring has been widely used for detecting myocardial ischemia in patients with unstable coronary syndromes [1]. For bedside monitors that allow continuous monitoring by means of the 12-lead ECG, the sensitivity and specificity of detecting myocardial ischemia can be improved by making better use of information provided by the available ECG leads. Lux *at al.* [2] hypothesised that BSPMs estimated from reduced lead sets (such as the 12-lead ECG) can provide more information than the predictor leads themselves, with the estimation method that incorporates prior knowledge derived from the large BSPM datasets.

In the previous study [3], we used general transformation to calculate BSPMs from the 12-lead ECG as an intermediate step to estimating heart-surface potentials during PCI-induced ischemia. The aim of the present study was to investigate how much can estimation of BSPMs from the 12-lead ECG be improved by using patient-specific [4] instead of general transformations.

2. Methods

2.1. Patient population

The design set for developing the general transformation from the 12-lead ECG to BSPMs was the Dalhousie Superset consisting of 120-lead ECGs from 892 subjects, including 290 normal subjects, 318 patients with previous myocardial infarction and 284 patients with inducible ventricular tachycardia [4]. The test set consisted of 120-lead ECGs from the Dalhousie database, including 88 patients with single-vessel coronary artery disease who underwent elective PCI [5]. There were 3 subgroups consisting of: 31 patients whose left anterior descending (LAD) coronary artery was occluded, 35 with right coronary artery (RCA) occluded, and 22 with left circumflex (LCx) coronary artery occluded.

2.2. ECG acquisition and processing

The 120-lead ECG recordings of the Dalhousie Superset were each made for 15 consecutive seconds. ECGs were amplified, filtered (band pass from 0.025 to 125 Hz), multiplexed, and digitized at 500 Hz into 12-bit samples (with 2.5-μV LSB). The test set, consisting of 120-lead ECGs obtained during PCI, was acquired with the same electrode array and the same acquisition system as the Superset, except that the limb leads had electrodes at Mason-Likar [6] sites. Processing of all ECGs involved signal averaging; for the PCI set, 15-second episodes at the "baseline" and the "peak-inflation" states were selected and the ST measurements were made from

the averaged QRST complexes at the J point.

2.3. Derivation of transform coefficients

Coefficients for estimating BSPMs from the 12-lead ECG were derived by regression analysis, as described previously [4]. Briefly, a regression model was fitted to the given dataset, to obtain a statistical estimate V' of the instantaneous voltage V at a given estimated lead by fitting the linear regression equation without intercept

$$V' = \sum_{i=1}^{k} \beta_i V_i$$

to the recorded voltages V_i in k predictor leads (k = 8 for the 12-lead ECG). The problem is to find the best-fitting coefficients β_i for predictor leads i = 1, …, k by looking for such estimates of β_i that minimize the error sum of squares over all available data samples of the QRST interval for the entire design set (general coefficients) or for a given subject (patient-specific coefficients). A general-purpose regression procedure (*PROC REG*) from the SAS package [7] performed a least-squares solution to the linear regression problem. The coefficients that best fitted the data were then applied as constants to the ECG signals of predictor leads to obtain the estimated BSPMs. BSPMs at J point were analyzed in this study.

2.4. Comparison of potential distributions

BSPM distributions were compared by means of three measures of fit: a similarity coefficient (*SC*); an rms error (*RMS*); and a relative error (*RE*) for each of 352 nodes; for analysis, the means of 352 nodes were used. With the actual and estimated potentials denoted as V_i and V_i' for a given node i, the similarity coefficient between two QRST waveforms comprising n samples is a ratio:

$$SC = \frac{\sum_{i=1}^{n} V_i V_i'}{\sqrt{\sum_{i=1}^{n} \left(V_i\right)^2} \sqrt{\sum_{i=1}^{n} \left(V_i'\right)^2}} .$$

The root-mean-square error (*RMS*), in microvolts, and relative error (*RE*) are defined as follows:

$$RMS = \sqrt{\frac{1}{n} \sum_{i=1}^{n} (V_i - V_i')^2} \; ; \quad RE = \sqrt{\frac{\sum_{i=1}^{n} (V_i - V_i')^2}{\sum_{i=1}^{n} V_i^2}} .$$

2.5. Clinical scenarios tested

Since our test set contains ECGs for both "baseline" and "peak-inflation" states (when ECGs might undergo morphological changes due to induced ischemia), we envisaged 6 scenarios mimicking situations on hospital arrival of patients with suspected Acute Coronary Syndromes: (1) BB-scenario: baseline BSPMs estimated by using baseline coefficients; (2) BP-scenario: baseline BSPMs estimated by using peak-inflation coefficients; (3) BG-scenario: baseline BSPMs estimated by using general coefficients; (4) PP-scenario: peak-inflation BSPMs estimated by using peak-inflation coefficients; (5) PB-scenario: peak-inflation BSPMs estimated by using baseline coefficients; (6) PG-scenario: peak-inflation BSPMs estimated by using general coefficients.

2.6. Statistical analysis

To assess significance of differences in measures of fit achieved under 6 different scenarios, 15 pairwise differences were tested using the paired *t*-test and then adjusted for multiple comparisons by a Dunn-Sidak *t*-test. Unprotected p values yielded by the paired *t*-test were used to calculate protected P values as follows: $P = 1 - (1 - p)^{15}$; the differences were considered significant for $P < 0.05$.

3. Results

Table 1 summarizes results for reconstructing BSPM distributions under 6 scenarios, for the entire test set (n = 88), in terms of 3 measures of fit (*SC*, *RMS*, *RE*). For instance, estimates of BSPMs at peak-inflation state from the 12-lead ECG by means of general coefficients achieved *SC* of 92.39 ± 3.46 % (line 6); corresponding *SC* for estimates using patient-specific coefficients derived from the baseline-state ECGs was 96.58 ± 4.27 % (line 5); this change in degree of fit is highly significant (P < 0.0001) for this, as well as for the other 2 measures.

Table1. Measures of fit for BSPMs estimated from the 12-lead ECG under the six scenarios

	Mean	SD	Min	Max
SC-BB, %	99.64	0.36	96.94	99.95
SC-BP, %	97.39	2.33	86.28	99.79
SC-BG, %	92.34	2.96	81.83	96.94
SC-PP, %	99.67	0.32	97.88	99.96
SC-PB, %	96.58	4.27	62.94	99.83
SC-PG, %	92.39	3.46	77.60	98.93
RMS-BB, μV	6.77	1.97	4.01	13.52
RMS-BP, μV	20.86	12.29	8.13	104.12
RMS-BG, μV	46.80	11.69	22.32	79.54
RMS-PP, μV	6.98	2.07	3.43	12.59
RMS-PB, μV	26.43	13.39	9.16	87.53
RMS-PG, μV	50.40	12.08	29.74	85.91
RE-BB, %	6.45	2.34	2.70	19.17
RE-BP, %	19.69	11.70	5.92	86.43
RE-BG, %	42.57	8.64	29.25	69.63
RE-PP, %	6.12	2.40	2.35	14.75
RE-PB, %	22.41	10.75	5.93	75.45
RE-PG, %	42.16	9.16	18.93	78.64

SC, similarity coefficient; RMS, rms error; RE, relative error; tested

scenarios (BB, BP, BG, PP, PB, PG) are described in Sec. 2.5. Differences in degree of fit between scenarios BP vs. BG and PB vs. PG are for all 3 measures of fit highly significant ($P < 0.0001$).

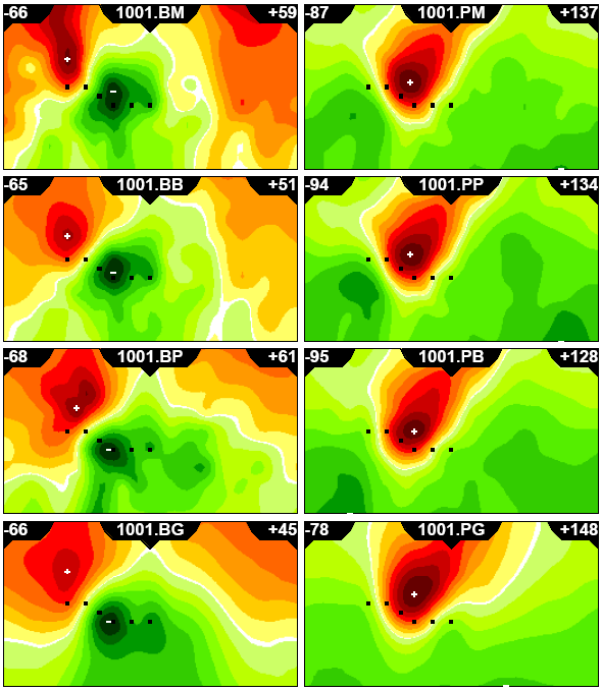

Figure 1. Actual and estimated BSPMs at J point for a patient whose LAD coronary artery was occluded. Left column shows baseline map constructed from 120 leads (BM) and 3-estimated baseline maps obtained under different scenarios (BB, BP, BG). Right column shows peak-inflation map constructed from 120 leads (PM) and 3 estimated peak-inflation maps (PP, PB, PG). Each map is shown on an unrolled cylindrical projection of the chest, with sites of 6 precordial leads marked. Max/min potential values are marked by +/– sign and their amplitudes (in microvolts) are in right/left corner of each map's panel; areas of positive/negative potentials are red/green, with 7 isopotential lines linearly spaced between zero and the larger extreme (max/min); note that this way of plotting emphasizes spatial patterns, including noise, in low-level distributions at the baseline state.

Figures 1–3 show for 3 randomly selected patients (identified by numbers 1001, 2001, and 3001, one from each test-set subgroup) how BSPMs reconstructed from 120 ECG leads (top row of each figure; BM, baseline map; PM, peak-inflation map) compare, in qualitative terms, with estimated BSPMs. For BSPM estimates under scenarios BB and PP, virtually perfect fit can be achieved; changes in spatial patterns that occur under the remaining scenarios (BP, BG, PB, PG) are subtle, but discernible by visual inspection. Figure 3 illustrates how peak-inflation ischemia caused by LCx coronary artery occlusion can be recognized by its spatial pattern of J-point potential distribution, even though the corresponding 12-lead ECG does not meet conventional STEMI criteria.

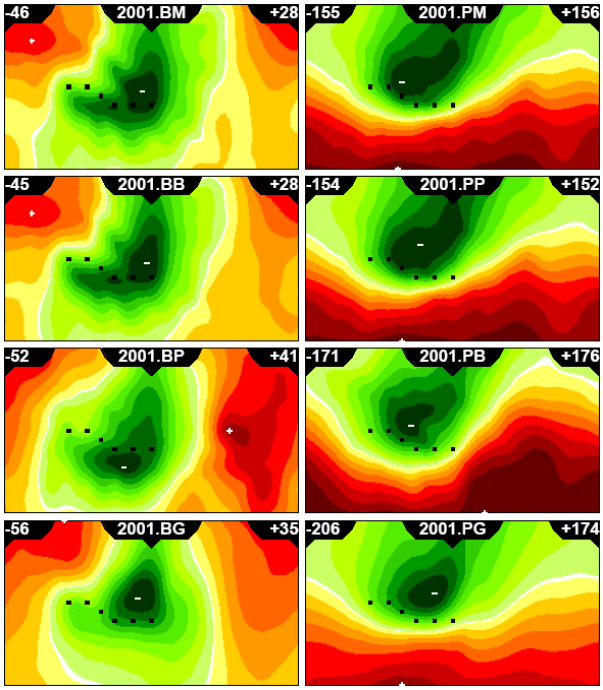

Figure 2. Actual and estimated BSPMs at J point for a patient whose RCA was occluded. Same layout as in Fig. 1.

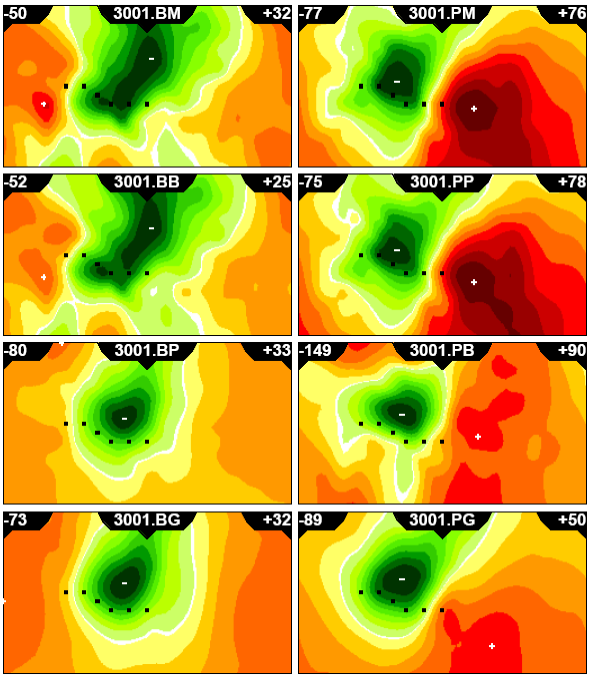

Figure 3. Actual and estimated BSPMs at J point for a patient with LCx coronary artery occluded. Same layout as Fig. 1.

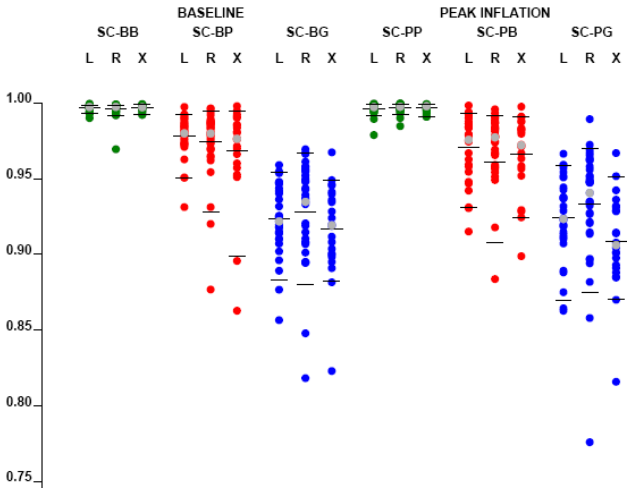

Figure 4. Similarity coefficient (*SC*) between actual BSPMs and those estimated from the 12-lead ECG for 6 scenarios (BB, BP, BG, PP, PB, PG) and 3 subgroups (L, LAD-occlusion group; R, RCA-occlusion group; X, LCx-occlusion group). Four scenarios (BB, BP, PP, PB) used patient-specific transformations, and two (BG, PG) used general transformations. Each colored circle represents *SC* value for one patient (one RCA outlier in the PB column with SC value less than 0.75 not shown); horizontal lines mark mean and 95% confidence limits for each subgroup; grey circles mark median values. Patient-specific transformations achieved significantly higher ($P < 0.0001$) *SC*s than general transformations in all subgroups.

Figure 4 shows distributions of *SC* values for individual patients of the 3 test-set subgroups, which were defined by occluded vessel. Statistical analysis found no significant differences among subgroups in any of 3 measures of fit. Thus, results for the entire test-set population (Table 1) are valid for any of the subgroups of Fig. 4.

4. Discussion

Two independent factors affect generation of body-surface ECGs: one involves primary bioelectric sources in the heart, and the other involves the effect of volume-conductor properties of extracardiac tissues. ECG lead transformations can only capture relationships among leads that depend solely on the second factor (in particular, on the shape and electrical properties of human torso). General transformations capture topological aspects of lead-to-lead relationships that are independent of torso size, whereas patient-specific transformations capture lead-to-lead relationships tailored for the particular patient's chest size and electrical properties (e.g., amount of fat, presence of edema). It stands to reason that the patient-specific transformations should yield better estimates of desired ECG leads. The question that remains to be answered, though, is: to what extent are patient-specific transformations invariant to changes in cardiac excitation sequence? Are the benefits of patient-specific transformations worth the extra effort required to apply them? Our results (see Fig. 4), obtained by the analysis of J-point BSPMs at baseline and peak-inflation states during balloon-inflation angioplasty, suggest that patient-specific transformations (red circles) are robust enough to give significantly better estimates of BSPMs than general transformations (blue circles), even when the cardiac sources change due to presence of ischemia (from baseline state to peak-inflation state and vice versa).

5. Conclusion

The results of this study show that, for patients with acute myocardial ischemia, BSPMs estimated from the 12-lead ECG by using both patient-specific and general transformations correlate well with those constructed from the 120 ECG leads. Thus this approach promises to be useful in ischemia detection and localization.

Acknowledgements

Support for studies at Dalhousie University was provided by the Heart & Stroke Foundation of Nova Scotia, by the Canadian Institutes of Health Research, and by the Philips Healthcare.

References

[1] Thygesen K *et al.* Universal definition of myocardial infarction: ESC/ACCF/AHA/WHF expert consensus document. *JACC* 2007;50:2173–95.

[2] Lux RL, MacLeod RS, Fuller M *et al.* Estimating ECG distributions from small numbers of leads. *J Electrocardiol* 1995;28(Suppl):92–8.

[3] Horáček BM, Warren JW, Wang JY. Heart-surface potentials estimated from 12-lead electrocardiograms. *Computing in Cardiology* 2010;37:37–40.

[4] Horáček BM, Warren JW, Wang JY. On designing and testing transformations for derivation of standard 12-lead/18-lead electrocardiograms and vectorcardiograms from reduced sets of predictor leads. *J Electrocardiol* 2008;41:220–9.

[5] Horáček BM, Warren JW, Penney CJ *et al.* Optimal electrocardiographic leads for detecting acute myocardial ischemia. *J Electrocardiol* 2001;34(Suppl):97–111.

[6] Mason RE, Likar I. A new system of multiple-lead exercise electrocardiography. *Am Heart J* 1966;71:196–205.

[7] *SAS User's Guide: Statistics*. SAS Institute Inc., Carey, NC, 1982.

Address for correspondence:
John Wang
Philips Healthcare
3000 Minuteman Road, MS-0455
Andover, MA 01810-1099
USA
E-mail: john.j.wang@philips.com